Acta Oceanol. Sin., 2023, Vol. 42, No. 4, P. 16–24
https://doi.org/10.1007/s13131-022-2111-4
http://www.aosocean.com
E-mail: ocean2@hyxb.org.cn

Sources and transformations of nitrite in the Amundsen Sea in summer 2019 and 2020 as revealed by nitrogen and oxygen isotopes

Yangjun Chen[1, 2], Jinxu Chen[1], Yi Wang[1], You Jiang[1], Minfang Zheng[1], Yusheng Qiu[1], Min Chen[1*]

[1] College of Ocean and Earth Sciences, Xiamen University, Xiamen 361102, China

[2] School of Marine Science and Fisheries, Jiangsu Ocean University, Lianyungang 222005, China

Received 29 June 2022; accepted 28 September 2022

Abstract

In this study, the nitrogen and oxygen isotope compositions of nitrite in the upper 150 m water column of the Amundsen Sea in the summer of 2019 and 2020 were measured to reveal the distribution and transformation of nitrite in the euphotic zone of the Southern Ocean. We found that primary nitrite maxima (PNMs) are widely present in the Amundsen Sea, where the depth of occurrence deepens from east to west and nitrite concentrations increases. Evidence from dual isotopes suggests that the formation of PNMs in all regions of the Amundsen Sea is dominated by ammonia oxidation. More importantly, the nitrogen and oxygen isotope compositions of nitrite in the Amundsen Sea mixed layer are abnormal, and their depth profiles are mirror symmetrical. Isotopic anomalies exhibit spatial variations, with central surface water having the lowest nitrogen isotope composition (–89.9‰±0.2‰) and western surface water having the highest oxygen isotope composition (63.3‰±0.3‰). Isotopic exchange reaction between nitrate and nitrite is responsible for these isotope anomalies, as both nitrogen and oxygen isotopes have large isotopic fractionation and opposite enrichment effects. This proves that isotopic exchange reaction operates extensively in different regions of the Amundsen Sea. Our study highlights the unique role of dual isotopes of nitrite in deepening the understanding of nitrogen cycle. Further studies on ammonia oxidation and isotopic exchange between nitrate and nitrite are warranted in the future to understand their roles in the nitrogen cycle in the Southern Ocean.

Key words: nitrogen isotope, oxygen isotope, nitrite, Amundsen Sea

Citation: Chen Yangjun, Chen Jinxu, Wang Yi, Jiang You, Zheng Minfang, Qiu Yusheng, Chen Min. 2023. Sources and transformations of nitrite in the Amundsen Sea in summer 2019 and 2020 as revealed by nitrogen and oxygen isotopes. Acta Oceanologica Sinica, 42(4): 16–24, doi: 10.1007/s13131-022-2111-4

1 Introduction

Nitrogen (N) is an essential nutrient needed for marine organisms to grow. Nitrate (NO_3^-), nitrite (NO_2^-) and ammonium/ammonia (NH_4^+/NH_3) are fixed N species available to organisms in the marine ecosystem, which greatly limit primary productivity in large parts of the ocean (Moore et al., 2013). Microbial-mediated biogeochemical processes involve multiple forms of N species and constitute a complex N cycle (Casciotti, 2016b; Hutchins and Capone, 2022).

NO_2^- is involved in almost all N biogeochemical processes, because it is not only a substrate for microbial metabolism in redox reactions, but also has abiotic activity that allows exchange of oxygen (O) atom with H_2O molecule (Buchwald et al., 2012; Buchwald and Casciotti, 2013; Casciotti et al., 2002, 2007). Despite its low concentration in seawater, the active biological and chemical activity of NO_2^- promotes its important role in N cycling. Stable accumulations of NO_2^- tend to occur at two depths in the ocean, one at or near the bottom of the euphotic zone, known as the primary NO_2^- maximum (PNM; Dore and Karl, 1996; Kiefer et al., 1976; Lomas and Lipschultz, 2006), and the other in the oxygen-deficient zone, known as the secondary NO_2^- maximum (Brandhorst, 1959; Codispoti et al., 1986). The accumulation of NO_2^- at these depths indicates a change in the microbially mediated N transformation process, resulting in production rates exceeding consumption rates with little effect from physical processes (Mackey et al., 2011). The biogeochemical processes affecting NO_2^- accumulation mainly include nitrification and assimilatory NO_3^- reduction in oxygenated water, and denitrification, anammox and NO_2^- oxidation in anoxic water. In oxygenated seawater, nitrification is both a source and a consumption of NO_2^-, thus playing a key role in the NO_2^- cycle. The nitrification process is mainly completed in two steps. The first step is to oxidize the organic remineralization product NH_4^+/NH_3 to NO_2^-, and the second step is to oxidize NO_2^- to NO_3^-. The product (NO_3^-) of the nitrification process is ultimately lost from the ocean as nitrous oxide (N_2O) and N_2 through denitrification and anammox (Casciotti, 2016b; Hutchins and Capone, 2022). Therefore, nitrification is an important link between sources and sinks of fixed N in the ocean. Since nitrification occurs in an aerobic environment, whereas denitrification and anammox occur in an anaerobic environment (Casciotti, 2016b; Hutchins and Capone, 2022), the link between them is generally considered to be indirect and

Foundation item: The Impact and Response of Antarctic Seas to Climate Change under contract Nos IRASCC 02-01-01 and IRASCC 01-01-02C; the National Natural Science Foundation of China under contract No. 41721005.
*Corresponding author, E-mail: mchen@xmu.edu.cn

with spatial and temporal variability. The two steps of nitrification are catalyzed by different microbes (Ward, 2008). The oxidation of NH_3 as the first step of nitrification is performed by NH_3-oxidizing bacteria (AOB) or archaea (AOA), which is the rate-limiting step of nitrification (Kowalchuk and Stephen, 2001). The oxidation of NO_2^- is catalyzed by NO_2^--oxidizing bacteria (NOB).

The Southern Ocean plays a pivotal role in oceanic nutrient cycling and climate change. For example, global cooling during the Late Pleistocene Ice Age was thought to have resulted from enhanced carbon storage in the Southern Ocean, thereby reducing atmospheric carbon dioxide (Chalk et al., 2017; Jaccard et al., 2013; Martínez-Garcia et al., 2011). One of the typical features in the Southern Ocean is that major nutrients such as NO_3^- and PO_4^- in surface waters are not completely exhausted by phytoplankton, which has been attributed to light or iron limitations (Martin et al., 1990; Mitchell et al., 1991). Several studies have been carried out on the N cycle in the upper layer of the Southern Ocean using stable isotopes, such as the reconstruction of the paleonutrients in the Southern Ocean (Altabet and Francois, 2001; DiFiore et al., 2006; Fripiat et al., 2019; Sigman et al., 1999), nitrification (DiFiore et al., 2009; Fripiat et al., 2014, 2015a, 2015b; Smart et al., 2015), new productivity (Froneman et al., 2001; Jochem et al., 1995; Mdutyana et al., 2020), and N isotope exchange between NO_3^- and NO_2^- in the Southern Ocean (Fripiat et al., 2019; Kemeny et al., 2016). In the Amundsen Sea, wind changes are driving more deep warm water to the shallower continental shelf (Naughten et al., 2022), leading to thinning of its ice shelves and rapid loss of the West Antarctic ice sheet (Shepherd et al., 2018; Bett et al., 2020; Naughten et al., 2022). These features make the Amundsen Sea an important area of the Southern Ocean closely related to global change. Revealing the biogeochemical characteristics of nitrogen in the Amundsen Sea is of great significance for a better understanding of the nitrogen cycle in the Southern Ocean.

Current research on the N cycle in the Southern Ocean has focused more on NO_3^-, and the understanding of the NO_2^- cycle is still very limited. The isotopic compositions of N and O in NO_2^- (represent as $\delta^{15}N_{NO_2^-}(‰) = [(^{15}N/^{14}N)_{NO_2^-}/(^{15}N/^{14}N)_{N_2} - 1]$ and $\delta^{18}O_{NO_2^-}(‰) = [(^{18}O/^{16}O)_{NO_2^-}/(^{18}O/^{16}O)_{VSMOW} - 1]$, respectively; VSMOW: Vienna Standard Mean Ocean Water) document processes related to production and consumption, thus providing the possibility to constrain biogeochemical cycles of NO_2^- (Buchwald and Casciotti, 2013; Casciotti, 2016b; Chen et al., 2021, 2022; Chen and Chen, 2022). In this study, the $\delta^{15}N_{NO_2^-}$ and $\delta^{18}O_{NO_2^-}$ in the upper waters of the Amundsen Sea in summer were measured to reveal the spatial distribution of dual isotopes in NO_2^- and PNMs, and their regulatory processes in different regions of the Amundsen Sea. Our study extends the dataset of NO_2^- dual isotopes in the Southern Ocean to contribute to a deeper understanding of the N cycle in the Southern Ocean.

2 Methods

2.1 *Sample collection*

Seawater samples were collected through China's 35th and 36th Antarctic Research Expeditions (CHINARE). During the 35th CHINARE conducted by R/V *Xuelong*, samples were collected from four sites at the Section A8 from January 16 to 19, 2019. During the 36th CHINARE conducted by R/V *Xuelong*, samples were collected from nine sites at the Sections A3 and RA2 from January 12 to February 5, 2020. Sections RA2, A3 and A8 are located in the western, central and eastern parts of the Amundsen Sea, respectively (Fig.1). Samples were collected from a 12 L Niskin bottle mounted on a Conductivity-Temperature-Depth (CTD) rosette. Only water samples above 150 m were collected for N and O isotopes analysis because the NO_2^- content in these samples was sufficient for isotopic measurement. Immediately after sample collection, 6 mol/L NaOH solution was added for preservation (Bourbonnais et al., 2015; Casciotti et al., 2007; Chen et al., 2021, 2022; Chen and Chen, 2022; Hu et al., 2016; Kobayashi et al., 2021). The fixed samples were stored at room temperature and brought to the onshore laboratory for subsequent analysis.

2.2 *Hydrochemical parameters*

Temperature and salinity were measured *in situ* by CTD probes on board (SBE 911plus, Sea Bird). The measurement accuracy of temperature and conductivity is 0.001℃ and 0.000 3 S/m, respectively. Chl *a* concentration was measured and calibrated directly from the probe equipped on the CTD.

The concentrations of NO_2^- and NH_4^+ were determined by the diazo-azo method and the sodium hypobromite oxidation method, and the detection limits were 0.02 μmol/L and 0.03 μmol/L, respectively.

2.3 *Nitrogen and oxygen isotopic composition in nitrite*

An optimized azide reduction method was used to simultaneously measure the N and O isotopic compositions in NO_2^- (Bourbonnais et al., 2015; Hu et al., 2016; McIlvin and Altabet, 2005). Considering the detection limit of the method, only samples with NO_2^- concentrations higher than 0.24 μmol/L were measured in this study. The procedure is detailed in Chen et al. (2021). Briefly, the maximum sample volume to transfer into a 20 mL headspace vial was determined from the NO_2^- concentration to yield the maximum N_2O production. The reagents and samples used were pre-purged with high-purity helium to remove possible N_2O gas. Sodium azide solution (2 mol/L) and acetic acid solution (7.8 mol/L) were prepared on the day of sample measurement and added to the sample in a 1:1 ratio (v/v) and mixed well. Buffer solution (0.9 mL) was added to the samples for the reaction. After about 1 h, 10 mol/L sodium hydroxide was added to terminate the reaction. The resulting N_2O gas was purified, enriched, and injected into an isotope ratio mass spectrometer (DELTA^{plus} XP, Thermo Fisher Scientific) for isotopic analysis. Standards for NO_2^- isotopes (RSIL-N23, RSIL-N7373, and RSIL-N10219; Casciotti et al., 2007) are measured by the same procedure as the sample to obtain the isotopic composition of the sample. The reaction volume for each sample and standard solution was kept consistent to minimize possible pH dependence in the azide reaction (Granger et al., 2020; Kobayashi et al., 2021). The nitrogen content of the standard was matched to that of the sample to

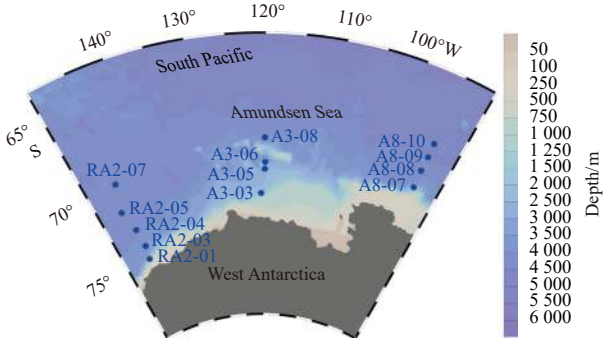

Fig. 1. Sampling locations in the Amundsen Sea in summer.

minimize the effect of sample size on NO_2^- isotope analysis. During the isotope measurement, every six samples were inserted into a set of standard solutions for simultaneous determination. The analytical precision for $\delta^{15}N$ and $\delta^{18}O$ in NO_2^- is better than 0.3‰ and 0.4‰ for samples and standards, respectively.

3 Results

3.1 *Hydrochemical characteristics*

3.1.1 *Characteristics of temperature and salinity*

The sea surface temperature (SST) in the Amundsen Sea ranged from –1.56℃ to 0.38℃, with the largest variation in the Section A8 in the east (Fig. 2a). The temperature minimum (T_{min}) and temperature maximum (T_{max}) appeared at different depths in sequence, with T_{min} at 50–200 m depth and T_{max} at 300–500 m depth (except RA2-03 at 1 000 m). Below T_{max}, the temperature gradually decreased and gradually became stable (Fig. 2d, gray line). T_{min} and T_{max} are ubiquitous features in the Southern Ocean (Altabet and Francois, 2001; Bindoff et al., 2000; DiFiore et al., 2009, 2010; Kemeny et al., 2016; Fripiat et al., 2019; Smart et al., 2015). The T_{min} reflects the characteristics of winter residual water retained in summer (Altabet and Francois, 2001; DiFiore et al., 2010), and the T_{max} reflects the influence of Circumpolar Deep Water (Bindoff et al., 2000; DiFiore et al., 2009; Fripiat et al., 2019).

The sea surface salinity in the Amundsen Sea varied between 32.68 and 33.97. Unlike the distribution of SST, the surface salinity in the three regions was relatively uniform. The salinity gradually increased with the increase of depth and stabilized below 500 m (Fig. 2e).

3.1.2 *Distributions of nitrite, ammonium and Chl a*

The NO_2^- concentration in the surface water of the Section RA2 was between 0.05 μmol/L and 0.31 μmol/L, with an average of 0.2 μmol/L (Fig. 2c, gray line). At the depth of 76 m at Station RA2-07 (which is also the depth of T_{min}), a subsurface peak of NO_2^- appeared with a concentration of 0.31 μmol/L (Fig. 2c, gray inverted triangle). At a depth of 200 m at all stations, NO_2^- was almost depleted (Fig. 2c). The NO_2^- concentration in water above 200 m in Section A3 was relatively uniform, ranging from 0.24 μmol/L to 0.27 μmol/L. The PNM appeared in the subsurface at Stations A3-03, A3-06 and A3-08 at a concentration of 0.24 μmol/L and at a depth of 74–76 m (Fig. 2c, blue line). Note that the NO_2^- concentration in the PNM of Section A3 was lower than that in Section RA2, but both occurred at similar depths (Fig. 2c). The NO_2^- concentration in the surface water of Section A8 was higher than that in the western and central surface water, and the highest is 0.41 μmol/L. PNM was also evident in Section A8, where the NO_2^- concentration was between 0.55 μmol/L and 0.65 μmol/L, and the occurrence depth was between 100 m and 150 m (Fig. 2c, yellow line). Compared with western and central PNMs, NO_2^- concentrations were higher in eastern PNMs, but the depth of occurrence was consistent. Similar to Sections RA2 and

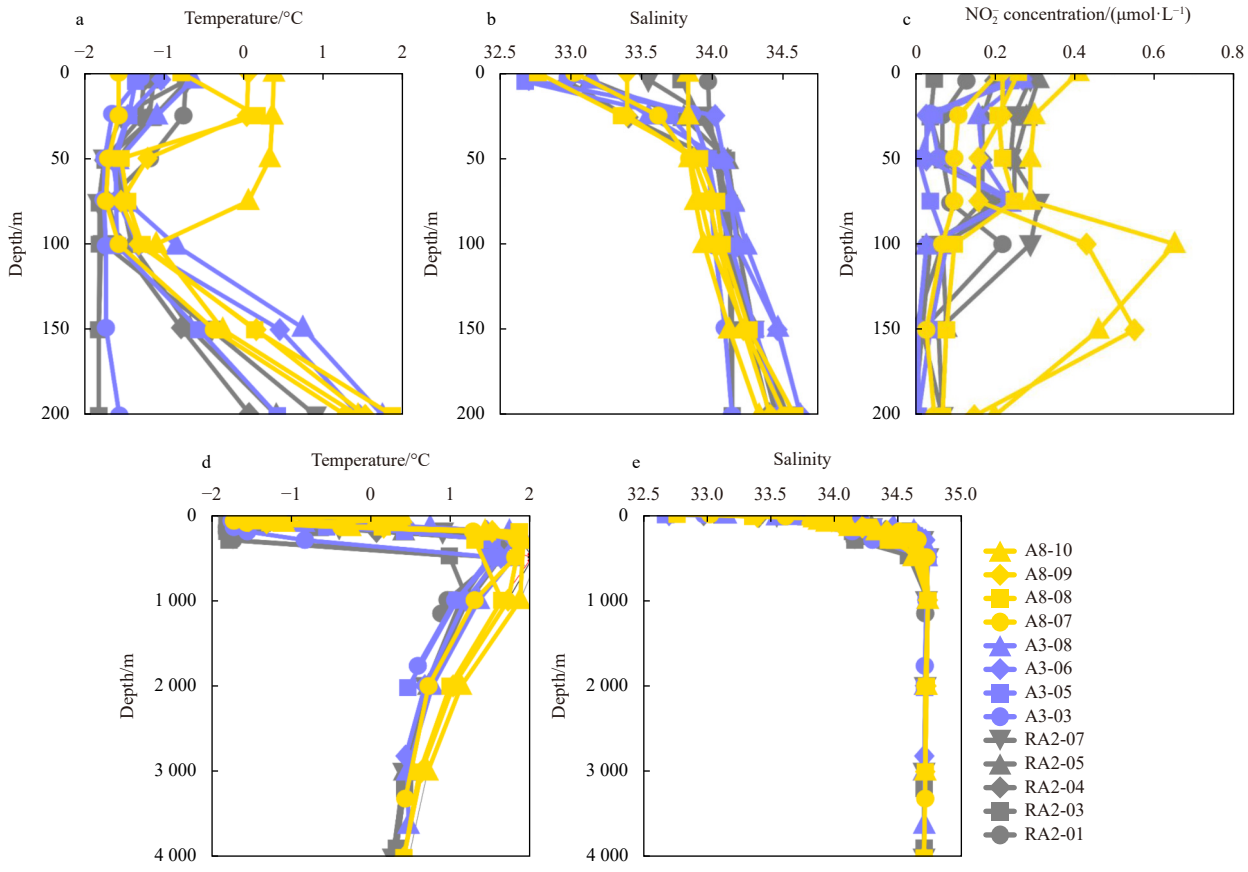

Fig. 2. Profiles of temperature, salinity and NO_2^- concentration at the Sections RA2 (gray line), A3 (blue line) and A8 (yellow line) in the Amundsen Sea. a and d are the temperature distributions in the water column above 200 m and in the entire water column, respectively; b and e are the salinity distributions in the water column above 200 m and in the entire water column, respectively; c is the distribution of NO_2^- concentration in the water column above 200 m.

A3, the NO_2^- concentration in Section A8 decreased gradually below PNM (Fig. 2c).

The distribution of NH_4^+ and Chl *a* in the water column above 200 m in the three stations of Section A8 was shown in Fig. 3. The NH_4^+ concentration in the surface water ranged from 0.46 μmol/L to 0.92 μmol/L, with an average of 0.65 μmol/L. Notably, NH_4^+ exhibited a subsurface maxima (AM) at a depth of 75 m, with concentrations ranging from 0.85 μmol/L to 1.89 μmol/L (Fig. 3, green line). In addition, deep chlorophyll maxima (DCM) appeared at depths of 25–50 m at the three sites (Fig. 3, gray line). Apparently, DCM, AM, and PNM appeared sequentially with increasing depth in Section A8 in the eastern Amundsen Sea, which is consistent with some previous reports in the oceanic euphotic zone (Mackey et al., 2011; Santoro et al., 2013). The occurrence of PNM along with DCM and AM in our study areas implies that the accumulation of NO_2^- may be related to the biogeochemical processes driven by the remineralization of organic nitrogen.

3.2 *Nitrogen and oxygen isotopic compositions in nitrite*

3.2.1 *Section RA2*

In the Section RA2 in the western Amundsen Sea, due to the limitation of NO_2^- concentration, profiles of isotopic compositions at two sites, RA2-05 and RA2-07, were obtained. The $\delta^{15}N_{NO_2^-}$ in the surface water was extremely low, with a minimum of −68.5‰±0.2‰, which was 30.5‰ lower than the reported minimum value in the other oceanic euphotic zone (−38‰; Buchwald et al., 2015). In the water column above 100 m, $\delta^{15}N_{NO_2^-}$ increased with depth, and the highest reached −0.8‰±0.3‰ (Fig. 4a, gray line). The extremely low $\delta^{15}N_{NO_2^-}$ we observed is consistent with previously reported values in the Southern Ocean (Chen et al., 2022; Fripiat et al., 2019; Kemeny et al., 2016).

$\delta^{18}O_{NO_2^-}$ in the surface water was abnormally high at 57.2‰±0.3‰ (Fig. 4b, gray line), which is 33.3‰ higher than that reported in other oceanic regions (23.9‰; Liu et al., 2020). The profile

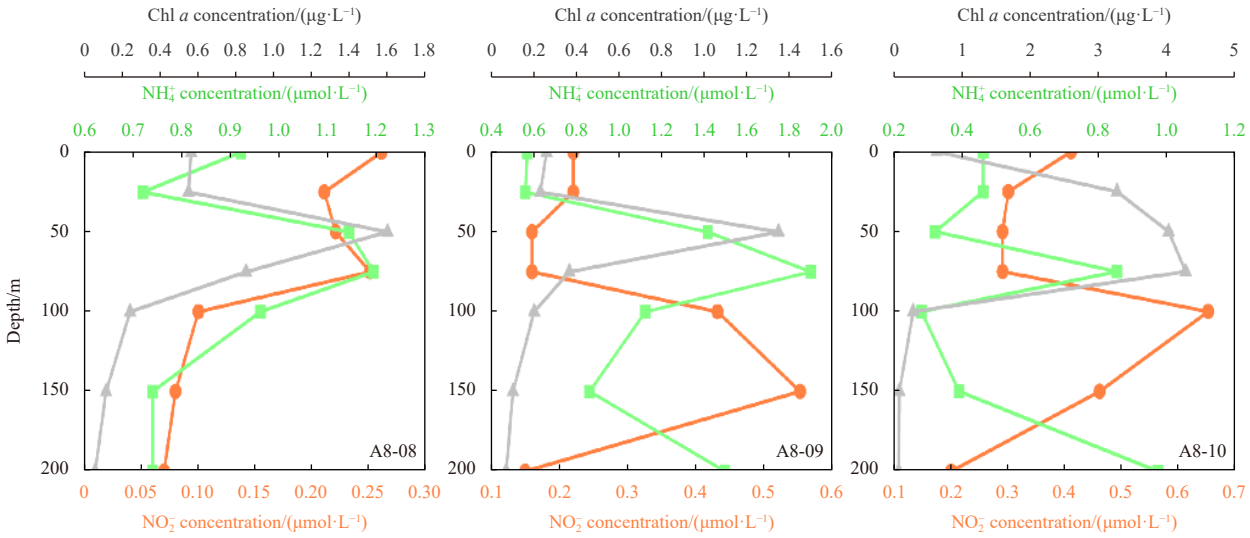

Fig. 3. Profiles of NO_2^-, NH_4^+, and Chl *a* in the upper 200 m water column at Section A8.

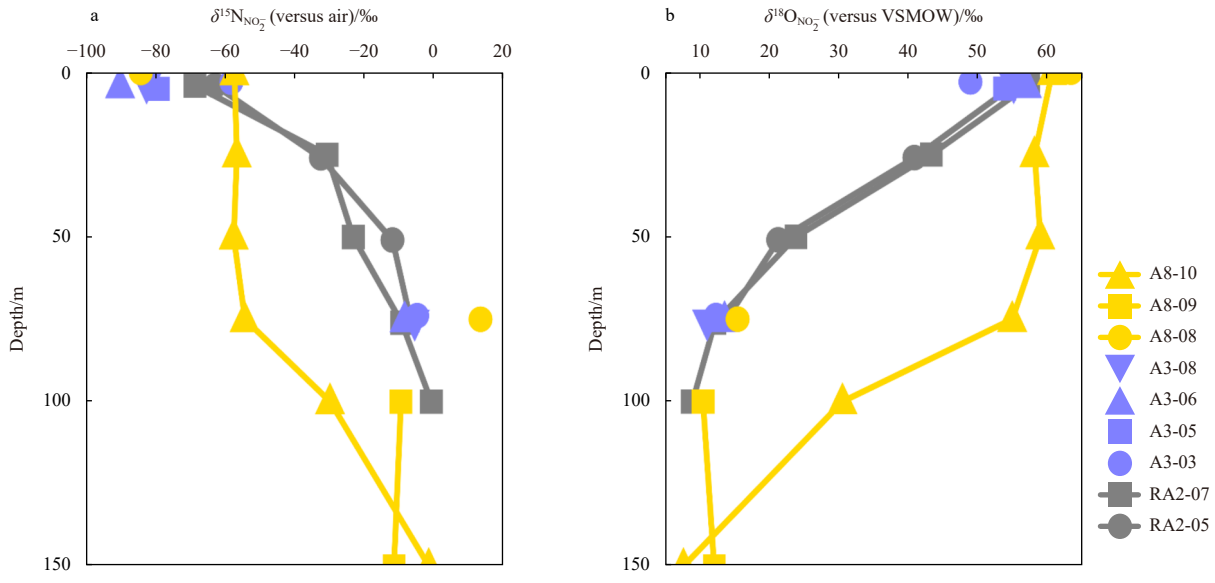

Fig. 4. Profiles of $\delta^{15}N_{NO_2^-}$ and $\delta^{18}O_{NO_2^-}$ in the Amundsen Sea. VSMOW: Vienna Standard Mean Ocean Water.

of $\delta^{18}O_{NO_2^-}$ showed a gradual decrease to 9.1‰±0.3‰ with increasing depth in the water column above 100 m, mirroring the variation of $\delta^{15}N_{NO_2^-}$ (Fig. 4). These features are consistent with previous results in the Amundsen Sea (Chen et al., 2022).

3.2.2 *Section A3*

In the Section A3 of the central Amundsen Sea, the $\delta^{15}N_{NO_2^-}$ in the surface water is also very low, with the lowest value of –89.9‰± 0.2‰, which is 13.0% lower than that of Section RA2. Although a complete profile was not obtained due to the limitation of low NO_2^- concentrations, a trend of increasing $\delta^{15}N_{NO_2^-}$ with depth was found (Fig. 4a, expressed in blue). The maximum $\delta^{15}N_{NO_2^-}$ (13.7‰±0.6‰) in Section A3 appeared at a depth of 75 m at Station A3-06, which was significantly higher than the maximum value in Section RA2 (–0.8‰±0.3‰).

The highest value of $\delta^{18}O_{NO_2^-}$ in the surface water in Section A3 is 57.0‰±0.2‰, which appeared at Station A3-06 with the lowest $\delta^{15}N_{NO_2^-}$ (Fig. 4b, blue triangle), and was also close to the highest value of $\delta^{18}O_{NO_2^-}$ in Section RA2. The $\delta^{18}O_{NO_2^-}$ in Section A3 roughly decreased with increasing depth, and the lowest value is 11.2‰±0.4‰ (Fig. 4b).

3.2.3 *Section A8*

The variation ranges of $\delta^{15}N_{NO_2^-}$ and $\delta^{18}O_{NO_2^-}$ in Section A8 in the Amundsen Sea are –84.0‰±0.2‰ to 13.3‰±0.2‰ and 7.8‰± 0.5‰ to 63.3‰±0.3‰, respectively. Similar to the other two sections, $\delta^{15}N_{NO_2^-}$ in Section A8 increased with depth, while $\delta^{18}O_{NO_2^-}$ decreased with depth (Fig. 4, expressed in yellow).

4 Discussion

4.1 *The importance of isotope exchange between nitrite and nitrate in regulating isotopic composition of nitrite*

In this study, the $\delta^{15}N_{NO_2^-}$ and $\delta^{18}O_{NO_2^-}$ in the upper 150 m water column of the Amundsen Sea in summer varied from –89.9‰ to 13.7‰ and from 7.8‰ to 63.3‰, respectively. These values are more anomalous than previous measurements of the Amundsen Sea (Chen et al., 2022). Compared with other oceanic reported values (Buchwald et al., 2015; Casciotti et al., 2013), the Amundsen Sea showed abnormally low $\delta^{15}N_{NO_2^-}$ and abnormally high $\delta^{18}O_{NO_2^-}$ values, reflecting that in addition to the traditional N cycle processes, other process may affect the isotopic composition of NO_2^- (Chen et al., 2022). In the traditional perspective of the N cycle, the N and O isotopic compositions of NO_2^- in the upper water are simultaneously affected by the generation and consumption processes of NO_2^-. The two generation processes of NO_2^- are NH_3 oxidation and assimilatory NO_3^- reduction, and the two consumption processes are NO_2^- oxidation and NO_2^- assimilation (Casciotti, 2016b; Hutchins and Capone, 2022). Here, we will estimate the range of possible variability of $\delta^{15}N_{NO_2^-}$ and $\delta^{18}O_{NO_2^-}$ in the Amundsen Sea under conventional N cycle regulation based on the isotope fractionation of these source and consumption processes, and then compare with our measurements to reveal other influencing process.

4.1.1 *Potential variation range of $\delta^{15}N_{NO_2^-}$ under conventional nitrogen cycling*

The theoretical range of $\delta^{15}N_{NO_2^-}$ from assimilatory NO_3^- reduction or NH_3 oxidation is assessed below. In the case where the NO_2^- is entirely derived from the assimilated NO_3^- reduction, the possible range of $\delta^{15}N_{NO_2^-}$ depended on the $\delta^{15}N$ in the NO_3^- and the replenished during the NO_3^- reduction. In the upper waters of the Southern Ocean, the $\delta^{15}N$ value in NO_3^- is 7.4‰ (Fripiat et al., 2019; Kemeny et al., 2016), and the N isotope effect in assimilatory NO_3^- reduction is 5‰ (Granger et al., 2004; Karsh et al., 2012). By assuming that NO_3^- has constant replenishment, consistent initial concentration and isotopic composition, and constant kinetic N isotope effects, it is estimated that the $\delta^{15}N_{NO_2^-}$ produced by assimilatory NO_3^- reduction was 2.4‰. This $\delta^{15}N_{NO_2^-}$ value can be altered by the process of NO_2^- consumption. Since the kinetic effect of N isotopes in phytoplankton assimilation of NO_2^- is about 0‰ (Waser et al., 1998), the $\delta^{15}N$ value in residual NO_2^- will remain at 2.4‰ if it is mostly consumed by phytoplankton assimilation. Differently, in the case where NO_2^- is mainly consumed by NO_2^- oxidation, the ^{15}N value of residual NO_2^- is estimated to be between –17.6‰ and –6.6‰, due to the reverse kinetic effect of N isotopes in NO_2^- oxidation ranging from –20‰ to –9‰ (Buchwald and Casciotti, 2010; Casciotti, 2009). Therefore, taking the above estimates together, the range of $\delta^{15}N_{NO_2^-}$ via assimilatory NO_3^- reduction is from –17.6‰ to 2.4‰. Similarly, potential changes in $\delta^{15}N_{NO_2^-}$ from NH_3 oxidation were estimated by kinetic fractionation effects of N isotopes during remineralization and NH_3 oxidation processes. Since $\delta^{15}N$ of NH_4^+ was not measured in this study, it is estimated by the $\delta^{15}N$ value of particulate organic nitrogen and the isotope effect of organic remineralization. The average $\delta^{15}N$ value of particulate organic nitrogen in the euphotic zone of the Southern Ocean is –2‰ (Lourey et al., 2003). We assumed that the $\delta^{15}N$ of NH_4^+ in the euphotic zone was 3‰ lower than that of particulate organic matter (Buchwald and Casciotti, 2013; Checkley and Miller, 1989; Lehmann et al., 2002; Macko et al., 1986; Peng et al., 2018), and thus estimated the $\delta^{15}N$ value of NH_4^+ to be –5‰. The fate of NH_4^+ in seawater has two main pathways, one is assimilation by phytoplankton, and the other is oxidation of NH_3. The fractionation effect of N isotopes in NH_3 oxidation is fully manifested in the case that most of the NH_4^+ is assimilated by phytoplankton and only a small part is oxidized to NO_2^- (Chen and Chen, 2022; Kemeny et al., 2016). Under this scenario, the $\delta^{15}N_{NO_2^-}$ value estimated from the kinetic N isotope effect (14‰–22‰; Casciotti et al., 2003) in NH_3 oxidation varies from –27‰ to –19‰. Another scenario is that NH_4^+ is mainly oxidized to NO_2^-. In this case, the $\delta^{15}N_{NO_2^-}$ estimated from the kinetic effect of N isotopes in the NH_4^+ assimilation by phytoplankton (about 0‰; Hoch et al., 1992; Vo et al., 2013) is close to the value of $\delta^{15}N_{NH_4^+}$ (i.e., –5‰). Meanwhile, $\delta^{15}N_{NO_2^-}$ produced by NH_3 oxidation is simultaneously affected by two NO_2^- consumption processes. In the case where NO_2^- is mainly assimilated by phytoplankton, the $\delta^{15}N$ value of residual NO_2^- remains unchanged, namely –5‰ or between –27‰ and –19‰. However, in the case where NO_2^- is mainly oxidized to NO_3^-, the $\delta^{15}N$ value of residual NO_2^- will be between –14‰ and –25‰ or between –47‰ and –28‰.

Combining the influences of the above conventional N cycle processes, the potential variation range of $\delta^{15}N_{NO_2^-}$ in the euphotic water in the Southern Ocean can be as low as –47‰ and as high as 2.4‰ (Fig. 5a, green shading).

4.1.2 *Potential variation range of $\delta^{18}O_{NO_2^-}$ under conventional nitrogen cycling*

As one of the sources of NO_2^-, NO_2^- produced by assimilatory NO_3^- reduction generally has a higher $\delta^{18}O$ value, because the branching oxygen isotope effect between NO_3^- and NO_2^- leads to the enrichment of ^{18}O in NO_2^- (Casciotti et al., 2007). According to the reported $\delta^{18}O$ value of NO_3^- in the euphotic zone of the Southern Ocean (3.7‰; Fripiat et al., 2019), kinetic effect of oxygen iso-

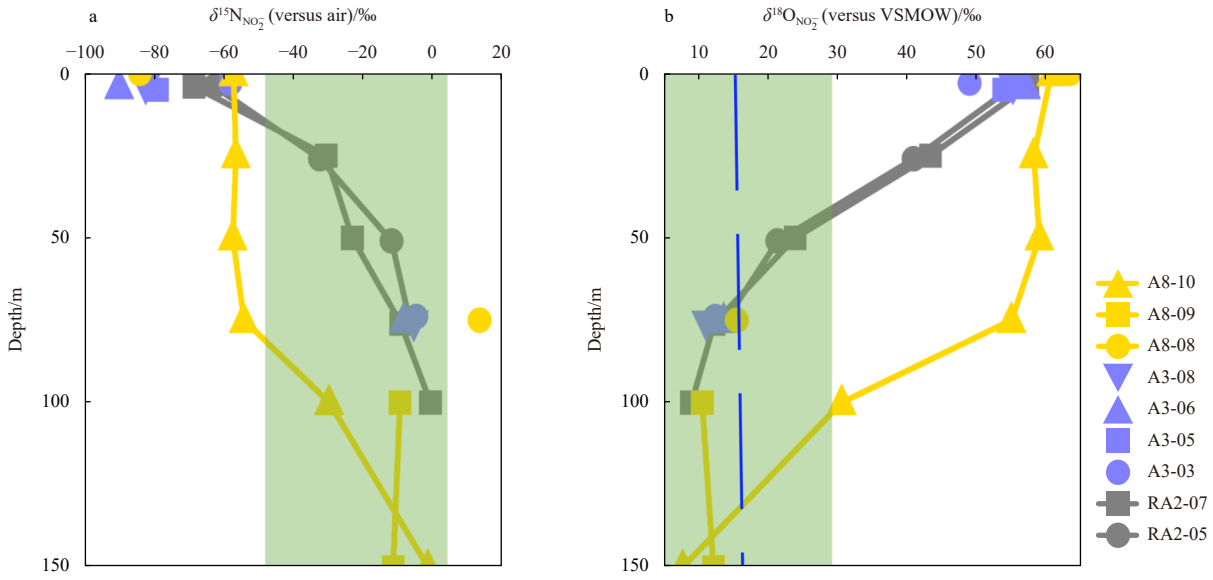

Fig. 5. $\delta^{15}N_{NO_2^-}$ and $\delta^{18}O_{NO_2^-}$ in water above 150 m in the Amundsen Sea and their influencing factors. Green shading indicates the potential variation range given by the conventional N cycle, blue dashed line indicates the value at which the O isotope exchange between NO_3^- and H_2O reaches equilibrium. VSMOW: Vienna Standard Mean Ocean Water.

topes (5‰; Granger et al., 2004; Karsh et al., 2012), and branching isotope effect (20‰–30‰; Casciotti et al., 2007), the $\delta^{18}O_{NO_2^-}$ produced by assimilatory NO_3^- reduction is estimated to fall between 18.7‰ and 28.7‰, with an average of 23.7‰. NO_2^- oxidation and assimilation of NO_2^- by phytoplankton may have an effect on $\delta^{18}O_{NO_2^-}$ values. When NO_2^- is mainly consumed by NO_2^- oxidation, it is estimated that the $\delta^{18}O$ value of residual NO_2^- may be reduced to between 10.7‰ and 27.7‰ based on the kinetic effect of O isotopes in the oxidation process (from −8‰ to −1‰; Buchwald and Casciotti, 2010). However, when NO_2^- is mainly consumed by phytoplankton assimilation, the $\delta^{18}O$ value of residual NO_2^- may be maintained between 18.7‰ and 28.7‰ due to the kinetic effect of O isotope close to 0‰ (Waser et al., 1998). Unlike $\delta^{15}N_{NO_2^-}$, $\delta^{18}O_{NO_2^-}$ is not only affected by biological processes but also by O isotope exchange between NO_2^- and H_2O (Buchwald and Casciotti, 2013; Casciotti et al., 2007). Based on the equation for the equilibrium effect of the exchange of O isotopes between NO_2^- and H_2O (Buchwald and Casciotti, 2013), the average equilibrium value of $\delta^{18}O_{NO_2^-}$ in water above 200 m in our study areas is estimated to be 15.6‰±0.1‰ from the *in situ* temperature. This means that if the biological turnover of NO_2^- is faster than the exchange of O isotopes between NO_2^- and H_2O, $\delta^{18}O_{NO_2^-}$ will be close to the biogenic characteristic (i.e., falling between 10.7‰ and 28.7‰), otherwise it will be close to the equilibrium value (15.6‰±0.1‰). The time scale for O isotope exchange equilibrium between NO_2^- and H_2O is typically weeks to months (Buchwald and Casciotti, 2013; Chen et al., 2021; Chen and Chen, 2022; Newell et al., 2011; Olson, 1981; Santoro et al., 2013; Ward et al., 1984). As the O isotope exchange proceeds, $\delta^{18}O_{NO_2^-}$ will eventually approach 15.6‰±0.1‰ (Fig. 5b, blue dotted line).

Estimating the potential range of $\delta^{18}O_{NO_2^-}$ produced by NH_3 oxidation is more complicated because NO_2^- incorporates O atoms from both H_2O and O_2 in the process (Buchwald et al., 2012; Casciotti et al., 2010), and O isotope exchange also occurs between NO_2^- and H_2O (Buchwald and Casciotti, 2013; Casciotti et al., 2007). According to the equation reported by Buchwald and Casciotti (2013), $\delta^{18}O_{NO_2^-}$ produced from NH_3 oxidation is estimated to be 2.9‰ under the assumption that the $\delta^{18}O$ value of seawater is –0.5‰ (Chen et al., 2022), the $\delta^{18}O$ value of dissolved oxygen is 24.2‰ (Buchwald and Casciotti, 2013), and the O atom exchange fraction between NO_2^- and H_2O is 0.08 (Buchwald et al., 2012). After further considering the influence of the two consumption processes of NO_2^-, the potential variation range of $\delta^{18}O_{NO_2^-}$ produced by NH_3 oxidation may be 2.9‰ or between –5.1‰ and 1.9‰.

Combining the influences of the above conventional N cycle processes, the potential variation range of $\delta^{18}O_{NO_2^-}$ in the euphotic zone of the Amundsen Sea may vary from –5.1‰ to 28.7‰ (Fig. 5b, green shading). In addition, no matter which biological process produces NO_2^-, when the O isotope exchange between NO_2^- and H_2O reaches equilibrium, $\delta^{18}O_{NO_2^-}$ will approach the equilibrium value (15.6‰±0.1‰, blue dotted line in Fig. 5b).

4.1.3 *Possible reasons for anomalous isotopic composition of nitrite*

According to the above isotopic fractionation of the traditional N cycle processes, in the upper water of the Southern Ocean, the variation range of $\delta^{15}N_{NO_2^-}$ is most likely between –47‰ and 2.4‰, and the highest $\delta^{18}O_{NO_2^-}$ is 28.7‰. However, the measured values of $\delta^{15}N_{NO_2^-}$ and $\delta^{18}O_{NO_2^-}$ in water above 150 m in the Amundsen Sea ranged from –89.9‰ to 13.7‰ and from 7.8‰ to 63.3‰, respectively. This means that the observed extremely low $\delta^{15}N_{NO_2^-}$ and extremely high $\delta^{18}O_{NO_2^-}$ cannot be fully explained by conventional biogeochemical processes of the N cycle (Chen et al., 2022). The samples deviating from the range of $\delta^{15}N_{NO_2^-}$ and $\delta^{18}O_{NO_2^-}$ expected by the conventional N cycle mainly occurred in the surface water and the water above 75 m at the three stations of Section A8, where the maximum gap of $\delta^{15}N_{NO_2^-}$ and $\delta^{18}O_{NO_2^-}$ reached –42.9‰ and 34.6‰, respectively (Fig. 5). This large difference implies that there may be an unknown process that alters $\delta^{15}N_{NO_2^-}$ and $\delta^{18}O_{NO_2^-}$, which may be presented throughout the upper water column, but only in these waters that are well expressed. Previous studies have speculated that there may be N isotope exchange between NO_3^- and NO_2^- in the Southern Ocean

driven by NOB's nitrite oxidoreductase (Chen et al., 2022; Fripiat et al., 2019; Kemeny et al., 2016). Kemeny et al. (2016) estimated the equilibrium effect of N isotopes in this exchange reaction to be between –69.2‰ and –59.9‰ based on the mass and isotopic balances of NO_3^- and NO_3^-+NO_2^-. Chen et al. (2022) calculated the equilibrium N isotope effect from $\delta^{15}N_{NO_2^-}$ measurements of –53.9‰±6.4‰. Clearly, the large isotopic fractionation in the N isotope exchange between NO_3^- and NO_2^- could well explain the extremely low $\delta^{15}N_{NO_2^-}$ values observed in this study. Similarly, the observed anomalously high $\delta^{18}O_{NO_2^-}$ can also be explained by isotope exchange reaction stemming from the large equilibrium O isotope effect in this process (37.6‰±3.5‰; Chen et al., 2022).

4.2 *Source of nitrite in the PNM*

The existence of PNM has been observed in the three sections of the Amundsen Sea (Fig. 2c). Here, we analyze the source of NO_2^- in these PNMs by using the N and O isotopic composition of NO_2^- to understand the formation mechanism of PNM in the Amundsen Sea.

The formation of PNM requires that the source of NO_2^- exceeds its consumption on a certain time scale. There are two possible sources of NO_2^- in PNMs of the Amundsen Sea, NH_3 oxidation and assimilatory NO_3^- reduction. As discussed above, the endmember values of $\delta^{15}N_{NO_2^-}$ and $\delta^{18}O_{NO_2^-}$ produced by assimilatory NO_3^- reduction are 2.4‰ and 23.7‰, respectively (Fig. 6, orange inverted triangle), while those produced by NH_3 oxidation are –5‰ and 2.9‰, respectively (Fig. 6, red square). Whichever source produces the NO_2^-, its exchange with water will cause the $\delta^{18}O_{NO_2^-}$ to approach the equilibrium value of 15.6‰± 0.1‰ (Fig. 6, thick horizontal dashed line). Therefore, in the case where NO_2^- is mainly provided by NH_3 oxidation, $\delta^{15}N_{NO_2^-}$ and $\delta^{18}O_{NO_2^-}$ will fall within the lower region surrounded by the NH_3 endmember line and the O isotope exchange equilibrium line

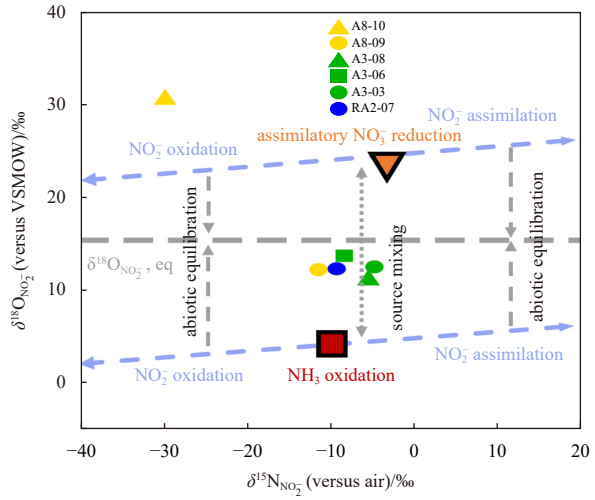

Fig. 6. The relationship between $\delta^{15}N_{NO_2^-}$ and $\delta^{18}O_{NO_2^-}$ in the PNM of the Amundsen Sea and associated biogeochemical processes (orange inverted triangle and red square represent endmember features produced by NH_3 oxidation and assimilatory NO_3^- reduction, respectively, and other color points represent our observed values. NO_2^- oxidation reduces $\delta^{15}N_{NO_2^-}$ and $\delta^{18}O_{NO_2^-}$ (Buchwald and Casciotti, 2010; Casciotti, 2009), while NO_2^- assimilation increases $\delta^{15}N_{NO_2^-}$ and $\delta^{18}O_{NO_2^-}$(Casciotti, 2016a), which is shown as a blue dashed line in the figure). VSMOW: Vienna Standard Mean Ocean Water.

(15.6‰±0.1‰). Conversely, in the case where NO_2^- is primarily provided by assimilatory NO_3^- reduction, $\delta^{15}N_{NO_2^-}$ and $\delta^{18}O_{NO_2^-}$ will fall within the upper region surrounded by the assimilatory NO_3^- reduction endmember line and the O isotope exchange equilibrium line (15.6‰±0.1‰) (Fig. 6).

Our results show that the vast majority of $\delta^{15}N_{NO_2^-}$ and $\delta^{18}O_{NO_2^-}$ data in PNMs in the Amundsen Sea fall in the lower region surrounded by the NH_3 endmember line and the O isotope exchange equilibrium line (Fig. 6), which proves that the source of NO_2^- is mainly from NH_3 oxidation. In addition, judging from the values of $\delta^{15}N_{NO_2^-}$ in PNMs in the Amundsen Sea may be mainly consumed by assimilation of phytoplankton. Otherwise, if NO_2^- oxidation dominates consumption, the large N isotope effect in the NO_2^- oxidation process will cause the $\delta^{15}N_{NO_2^-}$ value to be far away from the source signal (Fig. 6, red square). An exception is the $\delta^{15}N_{NO_2^-}$ and $\delta^{18}O_{NO_2^-}$ data in the PNM at Station A8-10, which is above the assimilatory NO_3^- reduction endmember line (Fig. 6, yellow triangle). Two possible reasons might explain this phenomenon. One explanation is that the $\delta^{18}O_{NO_2^-}$ value at this station was significantly higher than the equilibrium value (15.6‰± 0.1‰), implying that assimilatory NO_3^- reduction may be the main source of NO_2^-. Meanwhile, the $\delta^{15}N_{NO_2^-}$ significantly deviates from the endmember value of NO_2^- assimilation by phytoplankton, indicating that NO_2^- may be mainly consumed by NO_2^- oxidation. Another explanation is that $\delta^{15}N_{NO_2^-}$ and $\delta^{18}O_{NO_2^-}$ in the PNM at this station are partially influenced by the NO_3^--NO_2^- isotope exchange described above, resulting in a lower $\delta^{15}N_{NO_2^-}$ value and a higher $\delta^{18}O_{NO_2^-}$ value. However, further research is required to reveal the possible reasons.

The N and O isotopic compositions of NO_2^- suggest that NH_3 oxidation plays an important role in the formation of PNM in the Amundsen Sea, which further supports previous conclusions (Chen et al., 2022). Thus, the formation of PNMs in different regions of Amundsen Sea has a common source mechanism, which is consistent with the findings in the Ross Sea (Olson, 1981) and similar to the situation in other sea areas, such as the East Tropical North Pacific (Peng et al., 2015), the Arctic and subarctic oceans (Chen and Chen, 2022), the Arabian Sea (Buchwald and Casciotti, 2013; Newell et al., 2011), the South China Sea (Chen et al., 2021), the East China Sea (Liu et al., 2020), the central California Current (Santoro et al., 2013), the Sargasso Sea (Newell et al., 2013) and the Red Sea (Mackey et al., 2011). Although nitrification may be inhibited by light, it has been reported that AOA remains active under strong light (Smith et al., 2014). Therefore, NH_3 oxidation may play a key role in the formation of PNM in the global ocean (Chen and Chen, 2022).

5 Conclusions

Measurements of N and O isotopic compositions of NO_2^- in the upper 150 m water column in the Amundsen Sea in the summers of 2019 and 2020 showed that $\delta^{15}N_{NO_2^-}$ has abnormally low values and $\delta^{18}O_{NO_2^-}$ has abnormally high values, especially in surface water. The lowest value of $\delta^{15}N_{NO_2^-}$ and the highest value of $\delta^{18}O_{NO_2^-}$ reached –89.9‰ and 63.3‰, respectively. Spatially, the $\delta^{15}N_{NO_2^-}$ value in the central region of the Amundsen Sea is lower, while the $\delta^{18}O_{NO_2^-}$ value in three regions is relatively uniform. These outliers are beyond what can be explained by isotopic effects of traditional N conversion processes. Isotope exchanges between NO_3^- and NO_2^- with large isotopic effects and inverse changes in N and O isotopes have been proposed to be responsible for these anomalous values. The mirror changes in the $\delta^{15}N_{NO_2^-}$ and $\delta^{18}O_{NO_2^-}$ profiles support the possibility of this iso-

tope exchange reaction. Regardless of the effect of the isotopic exchange between NO_3^- and NO_2^-, the relationship between $\delta^{15}N_{NO_2^-}$ and $\delta^{18}O_{NO_2^-}$ shows that the data in PNMs are mostly close to the endmember characteristics of NH_3 oxidation and deviate from assimilatory NO_3^- reduction, indicating that NH_3 oxidation plays an important role in the formation of PNM in the Amundsen Sea. Future research needs to reveal whether the isotope exchange between NO_3^- and NO_2^- is widespread in the Southern Ocean. Further applying of the dual isotopes of NO_2^- is necessary to deepen our understanding of N cycle in the Southern Ocean.

Acknowledgements

We would like to thank Libao Gao's group at First Institute of Oceanography, Ministry of Natural Resources for providing data on *T*, *S* and Chl *a* concentration, and Jianming Pan's group at Second Institute of Oceanography, Ministry of Natural Resources for providing data on NO_2^- and NH_4^+. Thanks to R/V *Xuelong* and R/V *Xuelong 2* for their assistance in sample collection.

References

Altabet M A, Francois R. 2001. Nitrogen isotope biogeochemistry of the Antarctic Polar Frontal Zone at 170°W. Deep-Sea Research Part II: Topical Studies in Oceanography, 48(19–20): 4247–4273

Bett D T, Holland P R, Garabato A C N, et al. 2020. The impact of the Amundsen Sea freshwater balance on ocean melting of the west Antarctic ice sheet. Journal of Geophysical Research: Oceans, 125(9): e2020JC016305

Bindoff N L, Rosenberg M A, Warner M J. 2000. On the circulation and water masses over the Antarctic continental slope and rise between 80 and 150°E. Deep-Sea Research Part II: Topical Studies in Oceanography, 47(12–13): 2299–2326

Bourbonnais A, Altabet M A, Charoenpong C N, et al. 2015. N-loss isotope effects in the Peru oxygen minimum zone studied using a mesoscale eddy as a natural tracer experiment. Global Biogeochemical Cycles, 29(6): 793–811, doi: 10.1002/2014GB005001

Brandhorst W. 1959. Nitrification and denitrification in the eastern tropical North Pacific. ICES Journal of Marine Science, 25(1): 3–20, doi: 10.1093/icesjms/25.1.3

Buchwald C, Casciotti K L. 2010. Oxygen isotopic fractionation and exchange during bacterial nitrite oxidation. Limnology and Oceanography, 55(3): 1064–1074, doi: 10.4319/lo.2010.55.3.1064

Buchwald C, Casciotti K L. 2013. Isotopic ratios of nitrite as tracers of the sources and age of oceanic nitrite. Nature Geoscience, 6(4): 308–313, doi: 10.1038/ngeo1745

Buchwald C, Santoro A E, McIlvin M R, et al. 2012. Oxygen isotopic composition of nitrate and nitrite produced by nitrifying cocultures and natural marine assemblages. Limnology and Oceanography, 57(5): 1361–1375, doi: 10.4319/lo.2012.57.5.1361

Buchwald C, Santoro A E, Stanley R H R, et al. 2015. Nitrogen cycling in the secondary nitrite maximum of the eastern tropical North Pacific off Costa Rica. Global Biogeochemical Cycles, 29(12): 2061–2081, doi: 10.1002/2015GB005187

Casciotti K L. 2009. Inverse kinetic isotope fractionation during bacterial nitrite oxidation. Geochimica et Cosmochimica Acta, 73(7): 2061–2076, doi: 10.1016/j.gca.2008.12.022

Casciotti K L. 2016a. Nitrite isotopes as tracers of marine N cycle processes. Philosophical Transactions of the Royal Society A Mathematical, Physical and Engineering Sciences, 374(2081): 20150295

Casciotti K L. 2016b. Nitrogen and oxygen isotopic studies of the marine nitrogen cycle. Annual Review of Marine Science, 8: 379–407, doi: 10.1146/annurev-marine-010213-135052

Casciotti K L, Böhlke J K, McIlvin M R, et al. 2007. Oxygen isotopes in nitrite: analysis, calibration, and equilibration. Analytical Chemistry, 79(6): 2427–2436, doi: 10.1021/ac061598h

Casciotti K L, Buchwald C, McIlvin M. 2013. Implications of nitrate and nitrite isotopic measurements for the mechanisms of nitrogen cycling in the Peru oxygen deficient zone. Deep-Sea Research Part I: Oceanographic Research Papers, 80: 78–93, doi: 10.1016/j.dsr.2013.05.017

Casciotti K L, McIlvin M, Buchwald C. 2010. Oxygen isotopic exchange and fractionation during bacterial ammonia oxidation. Limnology and Oceanography, 55(2): 753–762, doi: 10.4319/lo.2010.55.2.0753

Casciotti K L, Sigman D M, Hastings M G, et al. 2002. Measurement of the oxygen isotopic composition of nitrate in seawater and freshwater using the denitrifier method. Analytical Chemistry, 74(19): 4905–4912, doi: 10.1021/ac020113w

Casciotti K L, Sigman D M, Ward B B. 2003. Linking diversity and stable isotope fractionation in ammonia-oxidizing bacteria. Geomicrobiology Journal, 20(4): 335–353, doi: 10.1080/01490450303895

Chalk T B, Hain M P, Foster G L, et al. 2017. Causes of ice age intensification across the mid-pleistocene transition. Proceedings of the National Academy of Sciences of the United States of America, 114(50): 13114–13119, doi: 10.1073/pnas.1702143114

Checkley Jr D M, Miller C A. 1989. Nitrogen isotope fractionation by oceanic zooplankton. Deep-Sea Research Part A: Oceanographic Research Papers, 36(10): 1449–1456

Chen Yangjun, Bardhan P, Zhao Xiufeng, et al. 2021. Nitrite cycle indicated by dual isotopes in the northern South China Sea. Journal of Geophysical Research: Biogeosciences, 126(7): e2020JG006129

Chen Yangjun, Chen Min. 2022. Nitrite cycling in warming Arctic and subarctic waters. Geophysical Research Letters, 49(12): e2021GL096947

Chen Yangjun, Chen Min, Chen Jinxu, et al. 2022. Dual isotopes of nitrite in the Amundsen Sea in summer. Science of the Total Environment, 843: 157055, doi: 10.1016/j.scitotenv.2022.157055

Codispoti L A, Friederich G E, Packard T T, et al. 1986. High nitrite levels off northern Peru: a signal of instability in the marine denitrification rate. Science, 233(4769): 1200–1202, doi: 10.1126/science.233.4769.1200

DiFiore P J, Sigman D M, Dunbar R B. 2009. Upper ocean nitrogen fluxes in the Polar Antarctic Zone: constraints from the nitrogen and oxygen isotopes of nitrate. Geochemistry, Geophysics, Geosystems, 10(11): Q11016

DiFiore P J, Sigman D M, Karsh K L, et al. 2010. Poleward decrease in the isotope effect of nitrate assimilation across the Southern Ocean. Geophysical Research Letters, 37(17): L17601

DiFiore P J, Sigman D M, Trull T W, et al. 2006. Nitrogen isotope constraints on subantarctic biogeochemistry. Journal of Geophysical Research: Oceans, 111(C8): C08016

Dore J E, Karl D M. 1996. Nitrification in the euphotic zone as a source for nitrite, nitrate, and nitrous oxide at station ALOHA. Limnology and Oceanography, 41(8): 1619–1628, doi: 10.4319/lo.1996.41.8.1619

Fripiat F, Elskens M, Trull T W, et al. 2015a. Significant mixed layer nitrification in a natural iron-fertilized bloom of the Southern Ocean. Global Biogeochemical Cycles, 29(11): 1929–1943, doi: 10.1002/2014GB005051

Fripiat F, Martínez-García A, Fawcett S E, et al. 2019. The isotope effect of nitrate assimilation in the Antarctic Zone: Improved estimates and paleoceanographic implications. Geochimica et Cosmochimica Acta, 247: 261–279, doi: 10.1016/j.gca.2018.12.003

Fripiat F, Sigman D M, Fawcett S E, et al. 2014. New insights into sea ice nitrogen biogeochemical dynamics from the nitrogen isotopes. Global Biogeochemical Cycles, 28(2): 115–130, doi: 10.1002/2013GB004729

Fripiat F, Sigman D M, Massé G, et al. 2015b. High turnover rates indicated by changes in the fixed N forms and their stable isotopes in Antarctic landfast sea ice. Journal of Geophysical Research: Oceans, 120(4): 3079–3097, doi: 10.1002/2014JC010583

Froneman P W, Laubscher R K, Mcquaid C D. 2001. Size-fractionated primary production in the South Atlantic and Atlantic sectors of

the Southern Ocean. Journal of Plankton Research, 23(6): 611–622, doi: 10.1093/plankt/23.6.611
Granger J, Boshers D S, Böhlke J K, et al. 2020. The influence of sample matrix on the accuracy of nitrite N and O isotope ratio analyses with the azide method. Rapid Communications in Mass Spectrometry, 34(1): e8569
Granger J, Sigman D M, Needoba J A, et al. 2004. Coupled nitrogen and oxygen isotope fractionation of nitrate during assimilation by cultures of marine phytoplankton. Limnology and Oceanography, 49(5): 1763–1773, doi: 10.4319/lo.2004.49.5.1763
Hoch M P, Fogel M L, Kirchman D L. 1992. Isotope fractionation associated with ammonium uptake by a marine bacterium. Limnology and Oceanography, 37(7): 1447–1459, doi: 10.4319/lo.1992.37.7.1447
Hu H, Bourbonnais A, Larkum J, et al. 2016. Nitrogen cycling in shallow low-oxygen coastal waters off Peru from nitrite and nitrate nitrogen and oxygen isotopes. Biogeosciences, 13(5): 1453–1468, doi: 10.5194/bg-13-1453-2016
Hutchins D A, Capone D G. 2022. The marine nitrogen cycle: new developments and global change. Nature Reviews Microbiology, 20(7): 401–414, doi: 10.1038/s41579-022-00687-z
Jaccard S L, Hayes C T, Martínez-García A, et al. 2013. Two modes of change in Southern Ocean productivity over the past million years. Science, 339(6126): 1419–1423, doi: 10.1126/science.1227545
Jochem F J, Mathot S, Quéguiner B. 1995. Size-fractionated primary production in the open Southern Ocean in austral spring. Polar Biology, 15(6): 381–392
Karsh K L, Granger J, Kritee K, et al. 2012. Eukaryotic assimilatory nitrate reductase fractionates N and O isotopes with a ratio near unity. Environmental Science & Technology, 46(11): 5727–5735
Kemeny P C, Weigand M A, Zhang R, et al. 2016. Enzyme-level interconversion of nitrate and nitrite in the fall mixed layer of the Antarctic Ocean. Global Biogeochemical Cycles, 30(7): 1069–1085, doi: 10.1002/2015GB005350
Kiefer D A, Olson R J, Holm-Hansen O. 1976. Another look at the nitrite and chlorophyll maxima in the central North Pacific. Deep-Sea Research and Oceanographic Abstracts, 23(12): 1199–1208, doi: 10.1016/0011-7471(76)90895-0
Kobayashi K, Fukushima K, Onishi Y, et al. 2021. Influence of δ^{18}O of water on measurements of δ^{18}O of nitrite and nitrate. Rapid Communications in Mass Spectrometry, 35(2): e8979
Kowalchuk G A, Stephen J R. 2001. Ammonia-oxidizing bacteria: a model for molecular microbial ecology. Annual Review of Microbiology, 55: 485–529, doi: 10.1146/annurev.micro.55.1.485
Lehmann M F, Bernasconi S M, Barbieri A, et al. 2002. Preservation of organic matter and alteration of its carbon and nitrogen isotope composition during simulated and *in situ* early sedimentary diagenesis. Geochimica et Cosmochimica Acta, 66(20): 3573–3584, doi: 10.1016/S0016-7037(02)00968-7
Liu Sumei, Ning Xiaoyan, Dong Shuhang, et al. 2020. Source versus recycling influences on the isotopic composition of nitrate and nitrite in the East China Sea. Journal of Geophysical Research: Oceans, 125(8): e2020JC016061
Lomas M W, Lipschultz F. 2006. Forming the primary nitrite maximum: nitrifiers or phytoplankton?. Limnology and Oceanography, 51(5): 2453–2467, doi: 10.4319/lo.2006.51.5.2453
Lourey M J, Trull T W, Sigman D M. 2003. Sensitivity of δ^{15}N of nitrate, surface suspended and deep sinking particulate nitrogen to seasonal nitrate depletion in the Southern Ocean. Global Biogeochemical Cycles, 17(3): 1081
Mackey K R M, Bristow L, Parks D R, et al. 2011. The influence of light on nitrogen cycling and the primary nitrite maximum in a seasonally stratified sea. Progress in Oceanography, 91(4): 545–560, doi: 10.1016/j.pocean.2011.09.001
Macko S A, Estep M L F, Engel M H, et al. 1986. Kinetic fractionation of stable nitrogen isotopes during amino acid transamination. Geochimica et Cosmochimica Acta, 50(10): 2143–2146, doi: 10.1016/0016-7037(86)90068-2
Martin J H, Gordon R M, Fitzwater S E. 1990. Iron in Antarctic waters. Nature, 345(6271): 156–158, doi: 10.1038/345156a0
Martínez-Garcia A, Rosell-Melé A, Jaccard S L, et al. 2011. Southern Ocean dust-climate coupling over the past four million years. Nature, 476(7360): 312–315, doi: 10.1038/nature10310
McIlvin M R, Altabet M A. 2005. Chemical conversion of nitrate and nitrite to nitrous oxide for nitrogen and oxygen isotopic analysis in freshwater and seawater. Analytical Chemistry, 77(17): 5589–5595, doi: 10.1021/ac050528s
Mdutyana M, Thomalla S J, Philibert R, et al. 2020. The seasonal cycle of nitrogen uptake and nitrification in the Atlantic sector of the Southern Ocean. Global Biogeochemical Cycles, 34(7): e2019GB006363
Mitchell B G, Brody E A, Holm-Hansen O, et al. 1991. Light limitation of phytoplankton biomass and macronutrient utilization in the Southern Ocean. Limnology and Oceanography, 36(8): 1662–1677, doi: 10.4319/lo.1991.36.8.1662
Moore C M, Mills M M, Arrigo K R, et al. 2013. Processes and patterns of oceanic nutrient limitation. Nature Geoscience, 6(9): 701–710, doi: 10.1038/ngeo1765
Naughten K A, Holland P R, Dutrieux P, et al. 2022. Simulated twentieth-century ocean warming in the Amundsen Sea, west Antarctica. Geophysical Research Letters, 49(5): e2021GL094566
Newell S E, Babbin A R, Jayakumar A, et al. 2011. Ammonia oxidation rates and nitrification in the Arabian Sea. Global Biogeochemical Cycles, 25(4): GB4016
Newell S E, Fawcett S E, Ward B B. 2013. Depth distribution of ammonia oxidation rates and ammonia-oxidizer community composition in the Sargasso Sea. Limnology and Oceanography, 58(4): 1491–1500, doi: 10.4319/lo.2013.58.4.1491
Olson R J. 1981. ^{15}N tracer studies of the primary nitrite maximum. Journal of Marine Research, 39(2): 203–226
Peng Xuefeng, Fawcett S E, Van Oostende N, et al. 2018. Nitrogen uptake and nitrification in the subarctic North Atlantic Ocean. Limnology and Oceanography, 63(4): 1462–1487, doi: 10.1002/lno.10784
Peng Xuefeng, Fuchsman C A, Jayakumar A, et al. 2015. Ammonia and nitrite oxidation in the Eastern Tropical North Pacific. Global Biogeochemical Cycles, 29(12): 2034–2049, doi: 10.1002/2015GB005278
Santoro A E, Sakamoto C M, Smith J M, et al. 2013. Measurements of nitrite production in and around the primary nitrite maximum in the central California Current. Biogeosciences, 10(11): 7395–7410, doi: 10.5194/bg-10-7395-2013
Shepherd A, Ivins E, Rignot E, et al. 2018. Mass balance of the Antarctic Ice Sheet from 1992 to 2017. Nature, 558(7709): 219–222, doi: 10.1038/s41586-018-0179-y
Sigman D M, Altabet M A, McCorkle D C, et al. 1999. The δ^{15}N of nitrate in the Southern Ocean: consumption of nitrate in surface waters. Global Biogeochemical Cycles, 13(4): 1149–1166, doi: 10.1029/1999GB900038
Smart S M, Fawcett S E, Thomalla S J, et al. 2015. Isotopic evidence for nitrification in the Antarctic winter mixed layer. Global Biogeochemical Cycles, 29(4): 427–445, doi: 10.1002/2014GB005013
Smith J M, Chavez F P, Francis C A. 2014. Ammonium uptake by phytoplankton regulates nitrification in the sunlit ocean. PLoS ONE, 9(9): e108173, doi: 10.1371/journal.pone.0108173
Vo J, Inwood W, Hayes J M, et al. 2013. Mechanism for nitrogen isotope fractionation during ammonium assimilation by *Escherichia coli* K12. Proceedings of the National Academy of Sciences of the United States of America, 110(21): 8696–8701, doi: 10.1073/pnas.1216683110
Ward B B. 2008. Nitrification in marine systems. In: Capone D G, Bronk D A, Mulholland M R, et al., eds. Nitrogen in the Marine Environment. 2nd ed. San Diego: Academic Press, 199–261
Ward B B, Talbot M C, Perry M J. 1984. Contributions of phytoplankton and nitrifying bacteria to ammonium and nitrite dynamics in coastal waters. Continental Shelf Research, 3(4): 383–398, doi: 10.1016/0278-4343(84)90018-9
Waser N A D, Harrison P J, Nielsen B, et al. 1998. Nitrogen isotope fractionation during the uptake and assimilation of nitrate, nitrite, ammonium, and urea by a marine diatom. Limnology and Oceanography, 43(2): 215–224, doi: 10.4319/lo.1998.43.2.0215